Tiako P.F. (ed) *Automated Systems, Data, and Sustainable Computing*. Chronicle of Computing. OkIP
 https://doi.org/10.55432/978-1-6692-0001-7_10

Complementarity and Variability of Wind and Solar Energy in Complex Terrain

Radian Belu[a,*], Darko Koracin[b]

[a]*Southern University, 801 Harding Blvd, Baton Rouge, 70813, USA*
[b]*University of Split, Rudera Boskovica 31, Split, 210000, Croatia*

ABSTRACT

Wind and solar energy are expected to play a major role, in the near future electricity generation mix. However, wind and solar energy-based generation are intermittent and non-dispatchable, not being suitable to supply base-load electric power. Their greater penetration and grid integration are critical issues due to their inherent intermittency and variability. Moreover, there are strong evidence that wind and solar energy are showing complementary over appropriate time and space scales. This work investigates such spatiotemporal complementarity and variability as a means by which electricity planners, developers, and grid operators might advance uses and grid integration of wind energy. Over 14 years of synchronous wind velocity and solar radiation measurements at several sites, located in complex terrain of Nevada are used in this study. To do so we used auto-correlations and cross-correlations in wind speed and solar radiation time series, by applying detrended fluctuation analysis and detrended cross-correlation analysis.

Keywords: Wind, Solar Energy, Complementarity, Detrended Fluctuation Analysis, Cross-correlation

I. INTRODUCTION

Wind and solar energy are the most abundant and ubiquitous renewable energy resources (Belu & Koracin, 2013; 2015; Santos-Alamillios et al., 2012; Sioshansi and Denholm, 2013; Jereza al., 2013; Monforti et al., 2014), representing significant opportunities for electricity generation with little environmental impacts. Despite their availability, the widespread use of these sources for electricity production is not straightforward. The essential argument is not whether the electric generation, using these two renewable energy sources is wise in the long run but how to achieve a sustainable energy regime in which such generation type can play a significant role into electricity production mix. Standing in the way are nontrivial hurdles of reliability, source intermittency and variability, conversion efficiency, land use issues, and disparities in the economic development of world regions. Wind and solar resources vary appreciably over short periods such as hours and days and their dependability, analysis and assessments as energy sources require complex and novel scientific approaches (Monforti et al., 2014; Sales dos Anjos, Alves da Silva, Stosic & Stosic, 2015; Sioshansi & Denholm, 2013; Jereza al., 2013, Santos-Alamillios al., 2012).

The ever increasing energy technology advancements continue to enable the integration of solar and wind energy generation with the grid. However, attempts to incorporate larger renewable energy based generation are experiencing lengthening queues for connection to the transmission and distribution systems, technical challenges, grid operator opposition, or land issues. Renewable energy system integration poses unique challenges to the conventional power system operation and control, thus limiting their easy integration. First, renewable energy resources tend to be geographically dispersed, favorable sites may be far from load centers. Second, wind and solar energy sources are intermittent, with hourly, daily, and seasonally variabilities, hence, they may over or under produce from the grid perspective to which they are connected. A photovoltaic (PV) system is influenced by solar radiation variability and intermittence. Today, good solar radiation data and resource assessments are available for any area or location. Wind energy systems have also reached maturity, as well as the grid integration of large wind farms, including offshore sites. The wind resource assessment is a crucial aspect of developments and new methods are making significant contributions (Belu and Koracin, 2013; 2015). Accurate evaluations of the wind or solar energy availability are important steps in assessing the economic viability of any project. On the other hand, it is also important to assess the resources against specific electricity load demand to understand the contribution such resources can make toward displacing less environmentally friendly generation systems. Moreover, a major barrier for further deployment and grid integration of these renewable energy sources is the lack of reliable wind data and in combination with the solar radiation availability as well as their accurate power forecasting. It is therefore very important to assess the combined solar and wind energy resource and to understand the complementarity of the solar and wind energy availability against the electricity load demand for a particular area. Our study aims to characterize and analyze the variability, complementarity and correlations between solar and wind energy resources for a given geographical area, western Nevada. Moreover, our work confirms the complementary nature of these energy sources, depending heavily upon the geographical location. Our results show that sitting of wind and solar systems should be coordinated to get greater benefits from resource combination feeding the same grid.

II. WIND AND SOLAR ENERGY VARIABILITY AND COMPLMENTARITY

A. Data and Experiments

The data analyzed her were collected during the several campaigns, operated by the Desert Research Institute. One was run near the Tonopah in western Nevada from August 2003 to March 2008 and the other one near Carson City from 2006 to

* Corresponding author E-mail: radian_belu@subr.edu

2014 (Belu and Koracin, 2009; 2013; 2019). For the Tonopah experiment wind direction and speed data were measured at every 10 minutes at five levels (10 m, 20 m, 30 m, 40 m, and 50 m) at four 50 m instrumented towers. The wind speed and direction (10 m and 50 m levels, only) were measured in a horizontal plane, with three-cup anemometers and wind vanes. The accuracy of these wind measurements is 0.1 m/s for the range 5 m/s to 25 m/s. The wind velocity data were also collected from an 80 m tower, by using sonic anemometers was sampled at 20 Hz at four levels 10 m, 40 m, 60 m and 80 m (between 2007 and 2008). The wind velocity was measured at 80 m tower by sonic anemometer (20 Hz) and standard anemometer with 1-minumte average interval. Besides the wind velocity, air temperature, atmospheric pressure, humidity, and solar radiation were measured at surface weather station located near each tower base. The experiment goal was to analyze and assess the wind and solar energy potentials in this area of western Nevada. In second experiment, located in Reno-Carson City area, wind velocities were measured using sonic anemometers at two 60 m, one 40 m and one 30 m towers (Belu and Koracin, 2009; 2013; 2015; 2019). In the last experiment the towers were operated from 2006 until 2014, with the exception of the 30 m tower, operated form 2006 until the end of 2010. The tower instrumentation was similar with one described above. Wind velocities less than 0.5 m/s were recorded as calm. Before data statistical and spectral analysis, a data quality control was performed to remove outliers and to interpolate small data gaps that may be present. Overall, our data are of sufficient quality, with less than 3% of the data removed as outliers or unacceptable data, with notable exception of one of the 60 m tower, second experiment for which due to the equipment malfunction 2 months of data, summer 2012 were lost. Assessments of the wind and solar energy potentials at a particular site involves analyzing their characteristics, the probability distributions of the measured solar radiation, wind velocity, the maximum wind speed, the wind and solar energy variability and seasonality, cloudiness, hourly and diurnal variations. Usually wind and solar characteristics are studied by using the observed data probability distributions, such as: Weibull, Rayleigh, log-normal, beta or other probability distribution functions (Belu and Koracin, 2013; 2015).

B. Variability and Complmentarity

Complementarity notion has a long application history in physics, economics, biology or mathematics. Nobel laureate Niels Bohr introduced complementarity as a foundation for quantum physics, advocating its importance in disciplines beyond the physics. However it was received less attention in power engineering or renewable energy studies. Both solar and wind power generators are intermittent fluctuating energy sources. Solar radiation and power follows annual, seasonal and diurnal patterns, caused by the earth's rotation and its movement around the sun, disturbed by the weather events, e.g. clouds, fog, etc. Wind energy follows local wind patterns and variations caused by the weather fronts and local topography. Such intermittent and fluctuating energy generators have several impacts on the power system, operation, control, or stability. Our expectation is that co-locating wind and solar electricity generation can assure higher total and more constant combined power output, improving the stability and reliability, phasing out some of the inherent variability of these energy sources. Similar effects are expected, even with a more constant power output for renewable energy generators distributed on a larger geographical area. The variability and complementarity nature of solar radiation and wind speed were qualitatively noted, however with only a handful of studies attempting their quantitative characterization. Usually, correlation coefficients are employed to quantify the similarity between two time series, while correlograms are used to present their relationship in a visual manner. The correlation coefficient is unaffected by scaling of the two time series. When, the correlation coefficient is equal to 1 the time series are fully correlated, while when it is -1, they are fully anti correlated. It should also be noted that the higher the values of the correlation coefficients, the higher similarity between the two time series exists. To put in evidence the dynamical behavior of the wind speeds or solar radiations for time scales larger than one month, a moving average low pass filter was applied, as expressed by this relationship:

$$\overline{U_N}(k) = \sum_{i=k-\frac{N-1}{2}}^{i=k+\frac{N-1}{2}} u_i \qquad (1)$$

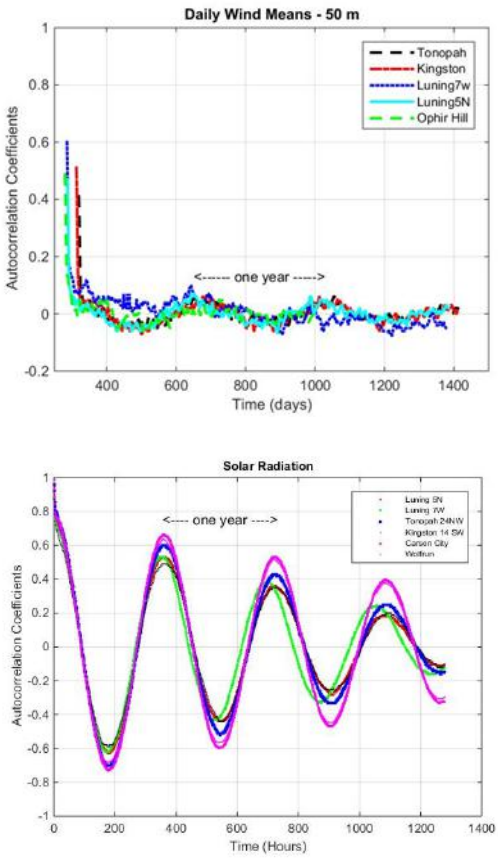

Fig.1. Autocorrelation of the daily mean wind speed and solar radiation, 2003-2014 composite data sets, all 50 m and 60 m towers (50 m and 60 m observation levels).

The moving averages corresponding to an averaging period of one month was computed for the solar radiation, wind velocity data measured at each site, and for all measurement levels, in the case of wind data. The one-month period was selected to capture

the annual and seasonal periodicities if any in the observed wind velocity and solar radiation time series. Fig. 1 (upper panel) shows the moving averages for Tonopah and Carson City towers, for the composite and overlapped 2003-2014 data sets. The wind speeds in diagrams of Fig. 1 were measured at 50 m and 60 m levels, respectively. Moving averages were computed using Eq. (1). Such plots are giving a first indication of the seasonal variations of the wind speed and solar radiation over the measurement sites. All graphs seem to indicate a typical annual cycle, with a wind speed maximum during the spring-summer season and with a minimum during the fall-winter season, while solar radiation is showing clear summer maximum and a winter minimum, as we are expecting for the semi-arid climate of Nevada. It is clear that a longer measurement period is required to further confirm this seasonality. The presence of a deterministic component with a period of about one year is clearly visible in these diagrams. Autocorrelations of daily solar radiation are showing more regular and large quasi-sinusoidal oscillations, while the peaks of wind and solar radiation are shifted about 100 days or so. The solar radiation yearly oscillations, as expected are better defined as the wind counterpart (lower panel diagram of Fig. 1). However, the complex terrain, local effects and other factors have stronger effects on the wind climatology, but still the diagram shows well defined quasi-annual oscillations in the daily wind speeds for all towers. Another result is the fairly good similarity of the variations of the large time scales for all the 50 m and 60 m towers. This is confirmed by the cross-correlation coefficients (Eq. 2), between the observation sites, defined by:

$$R_{xy}(\tau) = \begin{cases} \sum_{k=0}^{N-\tau-1} \frac{x_{k+\tau} y_k}{\sigma_x \sigma_y} & \tau > 0 \\ R_{xy}(\tau), & \tau < 0 \end{cases} \qquad (2)$$

where x and y are zero-mean stochastic variables, and σx and σy are their standard deviations. The computed values of the cross-correlation coefficients of the four 50 m towers, for smaller time lags are 0.6 or higher, showing a relative similarity in wind climatology. This is also a very strong indication of the stability and uniformity of the wind regimes in the western Nevada, an important characteristic for wind energy assessment, wind power plant operation, management and grid integration. Fig. 2 shows the auto-correlation functions of the wind speed and direction, at the 50 m, for the all four 50 m towers of the Tonopah experiment (2003-2008. It can be observed that all of these functions are coincidental, and are showing similar periodicity. A similar pattern in the auto-correlation functions was found for the other towers), including all towers of Reno-Carson experiment and at all measurement levels, even for shorter datasets. Regular oscillations exist, indicating that a well-defined periodicity characterizes the wind speed in western Nevada. A very slow decrease in the amplitude of the oscillation as the lag time τ increases indicates that the wind speed is not strictly periodic but is randomly modulated in frequency and phase. This behavior is also observed in the wind direction auto-correlation functions. The maintained oscillatory character of these functions indicates that the dominant frequencies associated with the wind speeds and directions are roughly coincidental. Similar patterns were found for all levels and towers, both for auto-correlations of wind speed and direction and for cross-correlations of wind speed and directions. This fact indicates that the wind speed and wind direction signals are very match in phase. It can be also be noted that the lag times corresponding to the maximum values of the auto-correlation functions are about 24 hours. This period of 24 hours as the dominant of the signals, shows that this is the time interval that basically governs the changes in wind speed and wind direction. This fact is related to the different behavior of the day and night winds which roughly maintain their structure during the almost 12 years of the time interval analyzed. We performed a similar analysis for solar radiation of all towers and locations, included in our project with available solar radiation observations.

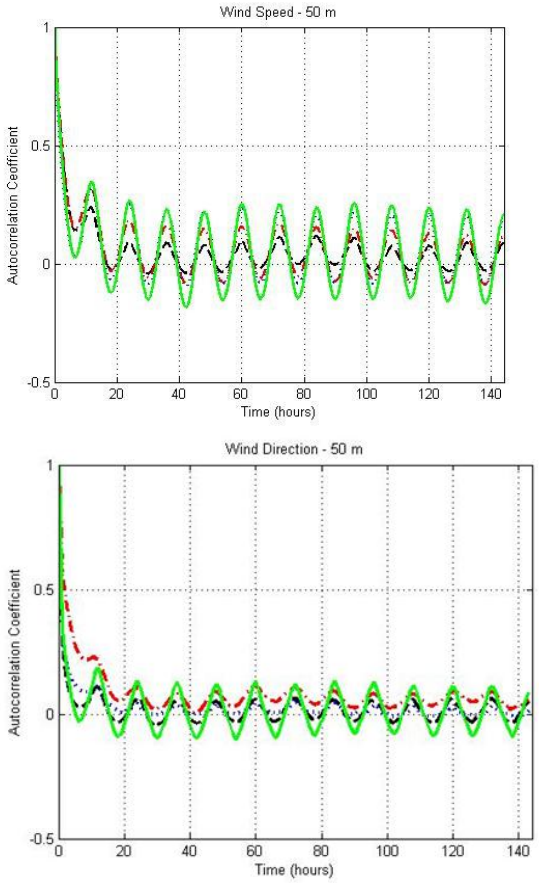

Fig. 2. Autocorrelation functions for the wind speed (upper panel) and the wind direction (lower panel) composite data sets, Tonopah experiment (2003 to 2008).

Two facts are immediately apparent in all of these autocorrelations. First, the presence of a strong sinusoidal component at diurnal frequency which is almost constant as the lag value increases indicating that it derives from a deterministic period component. While this pattern was expected in the solar radiation behavior, it is not so evident and expected in the wind speed time series. The second feature is that the centerline of the diurnal component is not the zero datum line, but is offset above the lag axis. This offset cannot be due to a zero mean (which is

removed by the autocorrelation algorithm), suggesting the presence of another periodic component of a much lower frequency. The obvious candidate for investigation is an annual cycle (Belu and Koracin, 2013; 2019). This agrees with the presence of a spring maximum and a fall minimum in the wind velocity moving average time series, as seen in Fig. 1.

C. Detrended Correlation and Cross-correlation Analysis

Detrended fluctuation analysis (DFA) is used in this work to quantify and compare correlations in wind speed and solar radiation time series. DFA method was introduced by Peng et al., 1996 for linear detrending, and extended since to higher order polynomials, being suitable to quantify long-term correlations in non-stationary signals or time series and has been employed in geophysics, meteorology, economy, medicine, etc. Detrended cross-correlation analysis (DCCA) was introduced by Podobnik and Stanley, 2008 to analyze power-law cross-correlations between two simultaneously recorded non-stationary time series. It has been subsequently extensively studied, and it has been successfully applied in the analysis of climatic, geophysical, and financial data, while on much lesser extend in the renewable energy (Belu & Koracin, 2019; Calif & Schmitt, 2014; Govidan & Kantz, 2004; Kiraly & Janosi, 2005; Malamund & Turcootte, 2006; Marinho, Sousa, & Andrade, 2013; Podobnik, Horvatic, Petersern, & Stanley, 2009; Suteanu, 2015). DFA method is an improvement of classical fluctuation analysis (Peng et al., 1996; Belu & Koracin, 2019). These methods, allowing determining the correlation properties on large time series are based on random walk theory. First, we compute the fluctuation time series or so-called 'profile' of a time series, (x_i), i = 1...N (with mean $\langle x \rangle = \sum_{i=1}^{N} x(i)$):

$$X(n) = \sum_{i=1}^{N} \left(x_i - \langle x \rangle \right) \quad (3)$$

The mean subtraction is not compulsory, since it is eliminated by the later detrending. The profile is then segmented into $N_S \equiv Int(N/s)$ non-overlapping segments or boxes of the same size ('scale') *s*. It is not critical that the time series size, N to be an integer multiple of scale, *s*, therefore short part of time series may exist at the end of the trajectory, *x(i)*. In order to acquire a high degree of accuracy in estimation process the forward procedure is applied from the opposite end (backward direction). Thereby, $2N_S$ segments are obtained. In each segment, we fit the integrated time series by using a linear regression or a higher-order polynomial function, the local trend subtracted to get the detrended fluctuation function.

$$x_s(k) = X(k) - p_v(k) \quad (4)$$

Here, $p_\nu(k)$ is the fitting polynomial in each segment. Linear, second order, cubic, or higher order polynomials can used in the fitting, usually called DFA_1, DFA_2, etc. We have to notice that the trends elimination in a series depends on the DFA order. After detrending, for each segment, the variance is found:

$$F^2(s,\nu) = \frac{1}{s}\sum_{i=1}^{s}\left\{X\left[(\nu-1)s+i\right] - p_v(i)\right\}^2 \quad (5)$$

For each segment $\nu = 1,....,N_S$ (forward direction) and

$$F^2(s,\nu) = \frac{1}{s}\sum_{i=1}^{s}\left\{X\left[N-(\nu-N_S)s+i\right] - p_v(i)\right\}^2 \quad (6)$$

The profiles are so computed for each segment $\nu = N_S+1,....,2N_S$ in the backward direction. Linear or higher order polynomials can be used in the fitting procedure. Then, the root-mean =-square fluctuation, F(s) is computed, as:

$$F(s) = \sqrt{\frac{1}{2N_S}\sum_{k=1}^{2N_S} x_s^2(k)} \quad (7)$$

Repeating this calculation for different segment (box) sizes provides the relationship between fluctuation function $F_{DFA}(s)$ and the segment size s. Typically $F_{DFA}(s)$ increases with s according to a power law [10-21]:

$$F_{DFA} \propto s^{\alpha} \quad (8)$$

In this way we obtained the average fluctuation *F(s)* as function the box or segment size, s. A linear relationship on a double logarithmic diagram reveals a scaling factor between those magnitudes, the slope of this line represents a scaling exponent. The scaling exponent α is obtained as the slope of regression (least square line fitting) of $\log[F_{DFA}(s)]$ vs. log(s). The value of $\alpha = 0.5$ indicates no correlation (white noise, uncorrelated signal), $\alpha > 0.5$ indicates persistent log-term correlations, while $\alpha < 0.5$ indicates persistent long-term anti-correlations. The values $\alpha = 1$ and $\alpha = 1.5$ correspond to 1/f noise and Brownian noise (integration of white noise) respectively.

There are situations that two or more variables are simultaneously recorded that can exhibit long-range dependence or multi-fractal nature, e.g. wind velocity, temperature, humidity, solar radiation, particulate concentration in turbulent flow, topographic indices and crop yield in agronomy, asset prices, indexes and trading volumes in financial market (Belu & Koracin, 2019; Calif & Schmitt, 2014; Govidan & Kantz, 2004; Kiraly & Janosi, 2005; Malamund & Turcootte, 2006; Marinho, Sousa, & Andrade, 2013; Podobnik, Horvatic, Petersern, & Stanley, 2009; Vasoler and Zebende, 2013; Zebebnde, 2011; Zebendea, da Silva, & Machado Filho, 2012). In recent years, the detrended cross-correlation analysis was proposed to investigate the long-range cross-correlations between two non-stationary time series. The DCCA method is a generalization of DFA method and is based on detrended covariance, being designed to investigate power-law cross-correlations between differently simultaneously recorded non-stationary time series. How we mentioned it has been extensively studied and applied in financial industry,

climatology, geophysics, and medicine. However, there are very few applications in solar and wind energy. The procedure consists of the integration of two simultaneously recorded time series x(i) and y(i), i = 1, , N to produce $X(k)=\sum_{i=1}^{k}x(i)$ and $Y(k)=\sum_{i=1}^{k}y(i)$, where k is an integer between 1 and N. The two integrated time series, X(k) and Y(k) are divided into N_S non-overlapping segments or boxes of equal length s. A linear (or higher order polynomial) is applied in each segments in order to capture the local trend, in similar way as applied in the DFA procedure. The integrated series X(k) and Y(k) are detrended by subtracting the local trends $X_{s,v}(k)$ and $Y_{s,v}(k)$ (the fitted polynomial ordinates within each segment $v = 1, \ldots, N_S$) from the data in each box or segment. Next the covariance of the residuals in each box is calculated:

$$F^2_{DCCA}(s)=\frac{1}{N-s}\sum_{i=1}^{N-s}f^2_{DCCA}(s,i) \quad (9)$$ If only a time series is considered $F^2_{DCCA}(s)$ reduces to the detrended variance $F^2_{DFA}(s)$ used in the DFA method, as discussed above. Repeating this procedure for several segment sizes, different scales, a relationship between $F_{DCCA}(s)$ and the segment size s is provided. If the series are power-law correlated, then $F_{DCCA}(s) \sim s^{\lambda}$ and λ is determined from linear regression of $\log\left[F_{DCCA}(s)\right]$ vs. $\log(s)$ with the same interpretation as α, the DFA exponent. However, to quantify the level of cross-correlation, we also computed the DCCA cross-correlation coefficient, defined as the ration between the detrended covariance, and the product of detrended variance function of each time series.

$$\rho_{DCCA}=\frac{F^2_{DCCA}(x_i,y_i)}{F_{DFA}(x_i)\cdot F_{DFA}(y_i)} \quad (10)$$

Its values are between -1 and 1, a value of ρ = 0, meaning no-correlations, and the above relationship leads to a new scale of cross-correlation in time series analysis.

III. RESULTS AND DISCUSSIONS

In order to get more inside on the complementarity and variability of the wind and solar energy resources in the study areas, we computed auto-, cross-correlation, DFA variance, DCCA covariance and DCCA cross-correlation coefficients for all wind and solar time series and for all available combinations of wind-wind, solar-solar and wind-solar of our time series. To verify the existence of linear trends and to estimate α, as well the use of DFA or higher order polynomials, we computed for each composite date sets (the time series for each site or tower), different DFA polynomial fittings, and similar for the DCCA method for all our composite data sets. Some of the results of the DFA analysis of wind speed and solar radiation time series are shown in Fig. 3 and are included in tables 1, 2 and 3. Both wind speed and solar radiation dynamics are showing good persistent properties (the coefficient α is higher than 0.5 for all analyzed time series and locations). The crossover point between the two scaling regions is found to be in the range, $1.4 \le x_0 \le 1.6$, corresponding to periodicity range between $10^{1.4} \approx 24$ h and $10^{1.6} \approx 48$ h. This is in very good agreement with our previous conventional correlation and autocorrelation analysis [5-7]. The wind speed dynamics and solar radiation are showing persistent and long-term correlation properties (α > 0.5) for all composite data sets, as shown in tables 1, 2 and 3.

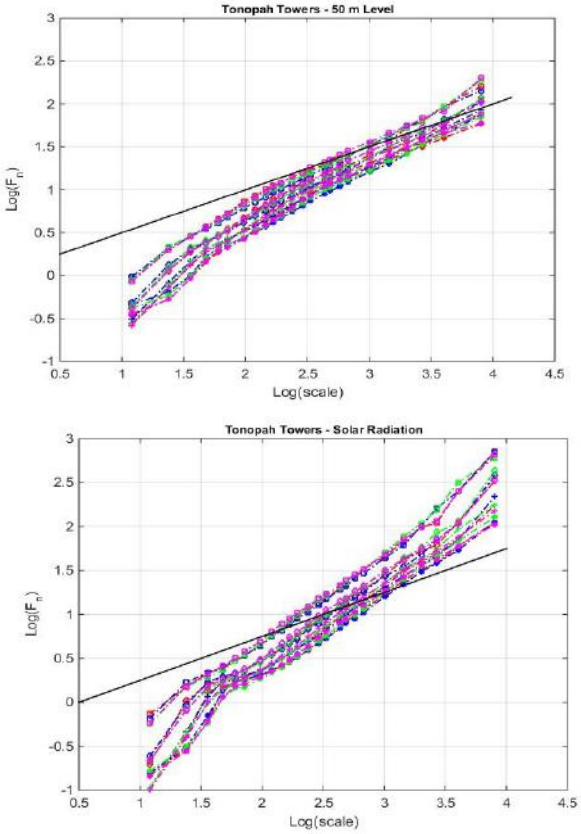

Fig. 3. DFA analysis of order 1, 2, 3, 4 and the 0.5 slope line of the hourly wind speeds for all 50 m towers and composite 2003-2008 data sets (upper panel) and solar radiation (lower panel)

IV. CONCLUSIONS

We analyzed the long-term correlations of wind speed and solar radiation time series recorded at several observation sites in Nevada, between 2003 and 2014. Both processes are characterized by long-term autocorrelations and persistent long-memory behavior. This property is also observed for a 365 day sliding windows, along the entire recorded period for each time series studied, however with, with different exponent values. Similar diurnal and seasonal periodicity we observed in the autocorrelations of all wind and solar time series, also in full agreement with our previous findings for Tonopah and Carson City experiments. Cross-correlations coefficients computed using regular statistical methods and DCCA analysis indicate

strong correlations between the wind and solar radiation data for each tower and measurement levels. However, the auto- and cross-correlations computed with DFA and DCCA have higher values suggesting a higher degree of complementarity between wind velocity and solar radiation data collected at different experimental locations, as well as over the study areas.

TABLE 1 DFA VARIANCES AND WUEBULL PARAMETERS FOR WIND SPEED DATA SETS

Tower Index	Period	Level (m)	DFA Variance	K	c(m/s)
T24NW	'03-'08	50	0.713	1.703	6.04
K14SW	'03-'07	50	0.705	1.415	4.82
L7W	'03-'08	50	0.716	1.346	4.39
L5N	'03-'08	50	0.746	1.335	3.99
Stone Cabin	'07-'08	60	0.885	1.667	5.92
Ophir	'06-'09	40	0.657	1.745	7.72
C-WT1	'08-'14	60	0.648	1.561	6.74
C-WT2	'08-'14	60	0.697	1.612	5.90
C-WT3	'09-'11	30	0.693	1.540	4.88

TABLE 2 DFA VARIANCES

Tower	Measurement Period	DFA Variance
T24NW	2003 – 2008	0.609
K14SW	2003 – 2008	0.604
L7W	2003 – 2008	0.616
L5N	2003 – 2008	0.639
Stone	2007 – 2008	0.702
Cabin	2009 – 2014	0.647
C-WT1	2009 – 2014	0.663
C-WT2		

TABLE 3 DCCA COVARIANCES, 50-m TOWERS 2003-2008 COMPOSITE DATA SETS (50 m LEVEL)

Towers	Tonopah 24NW	Kingston 14SW	Luning 7W	Luning 5N
T24NW	1.0000	0.807	0.723	0.831
K14SW	0.807	1.000	0.432	0.535
L7W	0.723	0.432	1.000	0.958
L5 N	0.831	0.535	0.958	1.000

ACKNOWLEDGMENT

We acknowledge support from the DOE-NREL, grant # (NDO 5-4431-01), and DOE Award #: NAX-9-66014-02 (DE-AC36-08G028308); DRI # 001523-008. DK was partially supported under the project STIM – REI, Contract Number: We thank Mr. Greg McCurdy of the Desert Research Institute, Reno, Nevada for helping with data acquisition.

REFERENCES

Alessio, E., Carbone, A., Castelli, G., & Frappietro, V., (2002). Second-order moving average and scaling of stochastic time series, Eur. Phys. J. B, 27, 197-200.

Belu, R., & Koracin, D. (2009). Wind Characteristics and Wind Energy Potential in Western Nevada, Renewable Energy, 34(10), 2246-2251.

Belu, R., & Koracin, D. (2013). Statistical and Spectral Analysis of the Wind Characteristics in the Western Nevada,J. of Wind Energy, 1, (12 pages), Article ID 739162, doi:10.1155/2013/739162.

Belu, R., & Koracin, D. (2015). Wind Energy Analysis and Assessment, Advances in Energy Research, 20(1), 1-55.

Belu, R., & Koracin, D. (2019). Regional Analysis of Wind Variability and Patterns in Complex Terrain," Geofizika, 36(2), 1-27, DOI: 10.15233/gfz.2019.36.6.

Calif R. & Schmitt F.G. (2014), Multiscaling and joint multiscaling description of the atmospheric wind speed and the aggregate power output from a wind farm. Nonlinear Processes in Geophysics, 21, 379-392.

Govindan, R. B., & Kantz, H. (2004). Long-term correlations and multifractality in surface wind speed. Europhysics Letters, 68, 184-190.

Hajian, S. M. & Sadegh, M., (2010). Multifractal Detrended Cross-Correlation Analysis of sunspot numbers and river flow fluctuations, Physica A, 389, 4942-4957.

Jereza, S., Trigo, R. M., Sarsa, A. Lorente-Plazas, R. Pozo-Vázquez, D., & Montávez, D. P., (2013). Spatio-temporal complementarity between solar and wind power in the Iberian Peninsula, Energy Procedia, 40, 48 – 57.

Kiraly, A., & Janosi, I. M. (2005). Detrended fluctuation analysis of daily temperature records: Geographic dependence over Australia, Meteorol Atmos Phys, 88, 119–128, DOI 10.1007/s00703-004-0078-7

Koscielny-Bunde E., Kantelhardt J. W., Braun P., Bunde A., & Havlin, S. (2006). Long-term persistence and multifractality of river runoff records: detrended fluctuation studies, J. Hydrol., 322, 120–137.

Malamud, B.D., & Turcotte, D. L. (2006). The applicability of power-law frequency statistics to floods. J Hydrololgy, 322, 168–180.

Marinho, E. B. S., Sousa, A. M., & Andrade, R.F. (2013). Using Detrended Cross-Correlation Analysis in Geophysical Data, Physica, A, 392, 2195-2201.

Monforti, F., Huld, T., Bódis, K., Vitali, L., D'Isidoro, M., & Lacal-Arántegui, R., (2014). Assessing complementarity of wind and solar resources for energy production in Italy. A Monte Carlo approach, Renewable Energy, 63, 576-586.

Oliveira Santos, M., Stosic, T. & Stosic, B., (2012). Long-term correlations in hourly wind speed records in Pernambuco, Brazil, Physica, A, 391, 1546-1552.

Peng, C. K. S. Havelin, S., Stanley, H., & Goldberger, A. (1995).Quantification of scaling exponents and crossover phenomena in nonstationary time series,Chaos, 5, 82–89.

Podobnik, B., & Stanley, H. E., (2008). Detrended Cross-Correlation Analysis: A New Method for Analyzing Two Nonstationary Time series, Phys. Rev. Lett., 100, 084102.

Podobnik, B., Horvatic, D., Petersen, M. A. & Stanley, H. E., (2009).Cross-correlation between volume change and price change, Proc. Natl. Acad. Sci., 106, 22079-22084.

Sales dos Anjos, P., Alves da Silva, A. S. Stosic, D. & Stosic, T. (2015). Long-term correlations and cross-correlations in wind speed and solar radiation temporal series from Fernando de Noronha Island, Brazil, Physica A, 424, 90-96.

Santos-Alamillios, F., Pozo-Vasquez, D. Ruiz-Arais, J. Lara-Fanego, V. & Tovar-Pescador, J., (2012). Analysis of Spatiotemporal Balancing between Wind and Solar Energy Resources in the Southern Iberian Peninsula, J. Applied Meteorology and Climatology, 51, 2005-2024.

Sioshansi, R. & Denholm, P. (2013). Benefits of Co-locating Concentrating Solar Power and Wind, IEEE Trans Energy Sustainability, 4(4), 877-885

Suteanu, C., (2015). A methodology for the time-scale-sensitive evaluation of wind speed and direction variability, Energy Procedia, 76, 200-206.

Vassoler, V. T. & Zebende, G. F., (2013). DCCA cross-correlation coefficient apply in time series of air temperature and air relative humidity,Physica A, 392, 1756-1761.

Zebende, G. F. (2011). DCCA cross-correlation coefficient: Quantifying the level of cross-correlation, Physica A, 390, 614-618.

Zebendea, G. F., da Silva, M. F., & Machado Filho, A., (2012). DCCA cross-correlation coefficient differentiation: Theoretical and practical approaches," Physica A, 391, 2438-2443.